CHEMISTRY
A EUROPEAN JOURNAL

DOI: 10.1002/chem.200600224

Silica-Coated Ln^{3+}-Doped LaF_3 Nanoparticles as Robust Down- and Upconverting Biolabels

Sri Sivakumar, Peter R. Diamente, and Frank C. J. M. van Veggel*[a]

Abstract: The preparation of nearly monodisperse (40 nm), silica-coated LaF_3:Ln^{3+} nanoparticles and their bioconjugation to FITC–avidin (FITC = fluorescein isothiocyanate) is described in this report. Doping of the LaF_3 core with selected luminescent Ln^{3+} ions allows the particles to display a range of emission lines from the visible to the near-infrared region ($\lambda = 450$–1650 nm). First, the use of Tb^{3+} and Eu^{3+} ions resulted in green ($\lambda = 541$ nm) and red ($\lambda = 591$ and 612 nm) emissions, respectively, by energy downconversion processes. Second, the use of Nd^{3+} gave emission lines at $\lambda = 870$, 1070 and 1350 nm and Er^{3+} gave an emission line at $\lambda = 1540$ nm by energy downconversion processes. Additionally, the Er^{3+} ions gave green and red emissions and Tm^{3+} ions gave an emission at $\lambda = 800$ nm by upconversion processes when codoped with Yb^{3+} ($\lambda_{ex} = 980$ nm). Bioconjugation of avidin, which has a bound fluorophore (FITC) as the reporter, was carried out by means of surface modification of the silica particles with 3-aminopropyltrimethoxysilane, followed by reaction with the biotin–*N*-hydroxysuccinimide activated ester to form an amide bond, imparting biological activity to the particles. A 25-fold or better increase in the FITC signal relative to the non-biotinylated silica particles indicated that there is minimal nonspecific binding of FITC–avidin to the silica particles.

Keywords: biolabels · lanthanides · nanostructures · silica · upconversion

Introduction

There is a large interest in the development of highly luminescent biomaterials for biological applications such as biolabelling, drug delivery, diagnostics of infectious and genetic diseases and so forth.[1] Materials such as traditional organic dyes,[2] quantum dots,[3] and metal nanoparticles[4] are widely applied in biological analyses but have some limitations. Organic dyes have a number of known drawbacks such as weak photostability, broad absorption and emission bands and toxicity.[2] Various semiconductor quantum dots display high photostability, size-dependent emissions, high quantum yields and narrow emission bandwidths, and have successfully been applied in biological applications.[3] However, the quantum dots are still controversial because of their inherent toxicity and chemical instability.[5] Moreover, their inherent short-lived luminescence lifetimes may overlap with the spontaneous background emission sources (natural fluorescence of biomolecules such as proteins is within 1–10 ns). Noble-metal nanoparticles (e.g., gold nanoparticles), which are known to scatter and absorb visible light, are potentially suitable candidates for biosensors.[4] Though these noble-metal nanoparticles are biocompatible, their optical properties in the visible region may overlap with natural proteins. Halas et al.[6] addressed this issue by developing a gold nanoshell over a silica sphere of submicron size for bioapplications such as the integration of cancer imaging and therapy. Notwithstanding this progress, there is still a need for more efficient biolabels with high photostability, biocompatibility, optical properties and ultrasensitivity to bioassays.

In order to address these key issues, the development of an alternative biomaterial through the use of lanthanide-doped nanoparticles is gaining popularity due to the latter's unique luminescence properties, such as sharp absorption and emission lines, high quantum yields, long lifetimes and superior photostability.[7] In particular, lanthanide ions are known to exhibit both efficient energy down- and upconversion emission properties, where the downconversion process is the conversion of higher energy photons into lower energy photons, which is also widely exploited in quantum

[a] S. Sivakumar, P. R. Diamente, Prof. Dr. F. C. J. M. van Veggel
University of Victoria
Department of Chemistry
P.O. Box 3065, Victoria
British Columbia V8W 3V6 (Canada)
Fax: (+1) 250-472-5193
E-mail: fvv@uvic.ca

WILEY InterScience DISCOVER SOMETHING GREAT
© 2006 Wiley-VCH Verlag GmbH & Co. KGaA, Weinheim

dots as well as in organic dyes.[8] In contrast, the upconversion process converts lower energy photons through multiphoton processes into higher energy photons, and is, in general, based on sequential absorption and energy-transfer steps.[9] One has to bear in mind that this event is different from multiphoton absorption processes, which typically require high excitation densities.[9]

At present, there are only a select number of reports on the use of lanthanide-based nanoparticles as potential biolabels that emit in the visible region, by either upconversion or downconversion processes.[5] Examples include the bioconjugation of Ln^{3+}-doped LaF_3 nanoparticles to avidin by our group,[10] and work done by Caruso and co-workers[11] with the functionalization of $LaPO_4$:Ce/Tb nanoparticles with streptavidin for biotin–streptavidin binding studies. In addition, a recent contribution from Li and co-workers[12] demonstrates that an Er^{3+}/Yb^{3+} upconverting nanoparticle label can be used in fluorescence resonant energy transfer (FRET)-type analyses, whereby the emission of the upconverting nanoparticles is quenched by the energy-accepting gold nanoparticles that are functionalised with biotin for biotin–avidin detection and quantification. Although these lanthanide-based articles prove the principle of bioconjugation, they have three main drawbacks. The first is long-term stability: it has been reported that ionic bound stabilising ligands can be pH-dependent and thus can be protonated off the surface of the nanoparticles in solution.[10] The second is toxicity due to exposure of lanthanide ions to the body, and finally, they emit only in the visible region. Only a few reports have dealt with these issues by developing a silica shell over the lanthanide-doped materials, such as silica-coated YVO_4:Eu nanoparticles functionalised with guanidinium for sodium channel targeting by Beaurepaire et al.,[13] and silica-coated Gd_2O_3:Tb nanoparticles functionalised with streptavidin by Louis et al.[14] Additionally, Niedbala and co-workers have made upconverting, silica-coated, lanthanide-doped submicron-sized ceramic particles for DNA assays.[15] The use of a silica coating over lanthanide-doped nanoparticles is an attractive alternative because the surface chemistry of silica spheres is well documented and silica is known to have benign effects in biological systems.[16] Upconverting and near-infrared (NIR)-emitting biolabels with a silica coating would be beneficial because upconverting materials can be excited with NIR light, which is outside the luminescent absorption range of biomolecules, thus minimising the loss of excitation energy to the surrounding material as compared with exciting with UV light.[5] Furthermore, excitation and emission in the NIR region can minimise interferences from the autofluorescence of proteins. However, these reports only showed emission in the visible region by a downconversion process, and to the best of our knowledge, there are no reports available on silica-coated lanthanide-doped nanoparticles that have both near-infrared ($\lambda = 750$–2000 nm) and upconverted emission.

Herein, we report a general and easy method for the preparation of silica-coated LaF_3:Ln nanoparticles and their bioconjugation to FITC–avidin (FITC = fluorescein isothiocyanate). These silica-coated nanoparticles display several non-overlapping emission lines that cover the visible to near-infrared region ($\lambda = 450$–1650 nm) through downconversion as well as upconversion processes, which can, for instance, be exploited in multiplexing applications.[17] The use of luminescent silica-coated LaF_3:Ln nanoparticles could have a number of advantages as probes in bioapplications over already existing biolabels:

1) LaF_3 has a very low phonon energy and therefore minimises the quenching of the excited-state lanthanide ions and thus has a high quantum yield.[7]
2) A wide range of emission lines ($\lambda = 450$–1650 nm) can be achieved by doping with selected lanthanide ions.
3) The codoping of the LaF_3 nanoparticle core with Yb^{3+} ions (for upconversion) makes it possible to excite with a light source at $\lambda = 980$ nm, which is outside the luminescent absorption range of biological molecules, thus minimising loss of excitation energy to the surrounding material as compared with exciting with UV light.
4) Excitation at $\lambda = 980$ nm of the codoped Yb^{3+} and Tm^{3+} nanoparticles produces an emission line at $\lambda = 800$ nm from Tm^{3+}; this wavelength is within the window ($\lambda =$ 700–1300 nm) in which skin and other biological materials are most transparent, as compared with UV-visible light, thus allowing for deeper penetration of excitation and easy escape of emitted light.[6]
5) Emission in the NIR region (from Yb^{3+}, Nd^{3+}, Er^{3+}) minimises interferences from the autofluorescence of proteins.
6) Silica is highly biocompatible and its surface chemistry is well documented for biological interactions.
7) The size of the silica shell can easily be adjusted to ease the secretion of nanoparticles through the kidney.
8) Longer luminescent lifetimes (μs to ms range) allow for gated time-resolved fluorescence. The consequence of these long lifetimes is that the photo count per second is low per single Ln^{3+} ion, but this is compensated for by the fact that we have many thousands of Ln^{3+} ions per nanoparticle.

Finally, non-size-dependent emissions (unlike quantum dots), completely stable photocycles and well-established Ln^{3+} doping procedures[7] make our approach attractive for preparing alternative biolabels.

Results and Discussion

The nanoparticle core matrices used to achieve the range of emission lines were as follows: $La_{0.95}Eu_{0.05}F_3$ (LaF_3:Eu), $La_{0.95}Tb_{0.05}F_3$ (LaF_3:Tb), $La_{0.95}Nd_{0.05}F_3$ (LaF_3:Nd), $La_{0.75}Yb_{0.20}Er_{0.05}F_3$ (LaF_3:Yb,Er) and $La_{0.75}Yb_{0.20}Tm_{0.05}F_3$ (LaF_3:Yb,Tm). First, the use of Tb^{3+} and Eu^{3+} ions resulted in green ($\lambda = 541$ nm) and red ($\lambda = 591$ and 612 nm) emissions, respectively, by energy downconversion processes. Second, the use of Nd^{3+} ions gave emission lines at $\lambda = 870$, 1070 and

 © 2006 Wiley-VCH Verlag GmbH & Co. KGaA, Weinheim

1350 nm and Er^{3+} ions gave an emission line at $\lambda = 1540$ nm by energy downconversion processes. Additionally, the Er^{3+} ions gave green and red emissions and Tm^{3+} ions gave an emission at $\lambda = 800$ nm by energy upconversion processes when codoped with Yb^{3+} ($\lambda_{ex} = 980$ nm). The surface of the silica-coated $LaF_3:Ln^{3+}$ nanoparticles was modified with 3-aminopropyltrimethoxysilane (APTMS), followed by reaction with biotin–*N*-hydroxysuccinimide for subsequent specific binding to FITC-labelled avidin (FITC–avidin), of which the FITC signal is monitored. The present work takes advantage of our recently published procedure to improve the upconversion and NIR emission of lanthanide ions in sol–gel-derived thin films (SiO_2, ZrO_2 and Al_2O_3), of which an important aspect is the effective separation of lanthanide ions from the high phonon-energy matrix, from residual OH groups and the absence of lanthanide-ion clustering.[18]

Shown in Scheme 1 is an outline of the step-wise preparation of the silica-coated $LaF_3:Ln^{3+}$ nanoparticles, starting from the citrate-stabilised $LaF_3:Ln^{3+}$ precursor nanoparticle

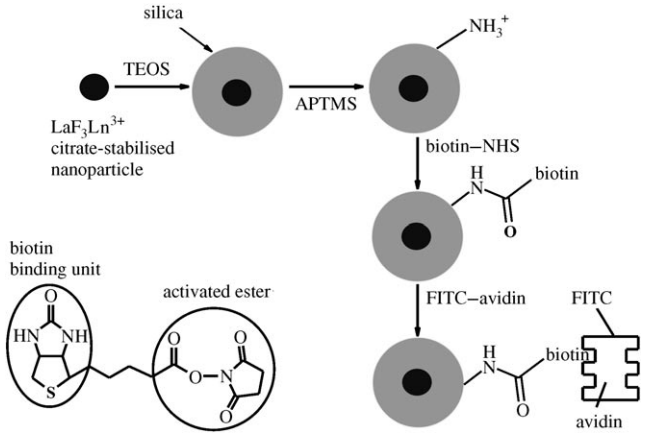

Scheme 1. Schematic illustration of the preparation and bioconjugation of silica-coated $LaF_3:Ln^{3+}$ nanoparticles to FITC–avidin (not to scale). APTMS = $(CH_3O)_3{-}Si{-}(CH_2)_3{-}NH_2$.

as the core matrix, followed by the formation of the silica shell by a modified Stöber process,[19] and then its subsequent bioconjugation to FITC–avidin. To further our earlier work on the improvement of the upconverted and NIR emission of lanthanide ions in sol–gel-derived thin films,[18] silica-coated LaF_3:Yb,Er, LaF_3:Yb,Tm and LaF_3:Nd (before surface modification with APTMS) nanoparticles were heated at 800 °C for 12 h to improve significantly their NIR luminescence as well as upconversion efficiency.

The transmission electron microscopy (TEM) image shown in Figure 1 is of the as-prepared silica-coated LaF_3:Nd nanoparticles, which clearly shows that almost all the silica beads have a single core LaF_3:Nd nanoparticle (≈ 5 nm) in their centre with an average shell thickness of ≈ 17 nm (± 5 nm). The LaF_3:Nd core has a slightly higher contrast than the silica shell. Figure 2a shows the emission spectrum of the as-prepared silica-coated LaF_3:Eu nanoparticles, in which the major emission bands of the Eu^{3+} ions at

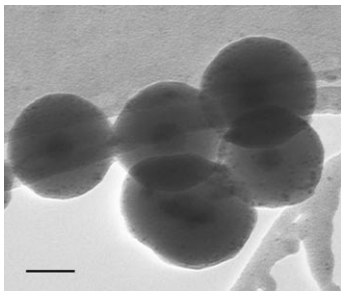

Figure 1. TEM image of as-prepared silica-coated LaF_3:Nd nanoparticles. Scale bar = 20 nm.

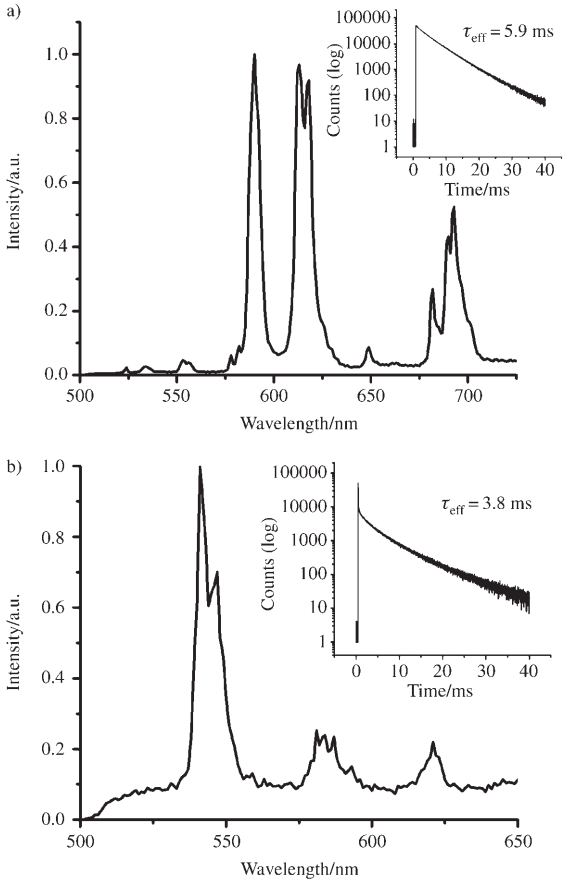

Figure 2. a) Emission spectra of as-prepared silica-coated LaF_3:Eu nanoparticles ($\lambda_{ex} = 464$ nm). Inset: decay curve for silica-coated LaF_3:Eu nanoparticles before surface modification ($\lambda_{ex} = 464$ nm, $\lambda_{em} = 591$ nm). b) Emission spectra of as-prepared silica-coated LaF_3:Tb nanoparticles ($\lambda_{ex} = 485$ nm). Inset: decay curve for silica-coated LaF_3:Tb nanoparticles before surface modification ($\lambda_{ex} = 485$ nm, $\lambda_{em} = 542$ nm). a.u. = arbitrary units.

$\lambda = 590$ and 612 nm are assigned to the $^5D_0 \rightarrow {}^7F_1$ and $^5D_0 \rightarrow {}^7F_2$ transitions. A detailed analysis of the emission spectrum has been reported by us elsewhere.[7a] The effective lifetime (defined in the Experimental Section) of 5.9 ms is from the $^5D_0$ level (inset in Figure 2a) with an estimated quantum yield of 88% based on the radiative lifetime of 6.9 ms.[7f]

 © 2006 Wiley-VCH Verlag GmbH & Co. KGaA, Weinheim

The emission spectrum of the as-prepared silica-coated LaF_3:Tb^{3+} nanoparticles is shown in Figure 2b, in which the most intense peak at $\lambda = 545$ nm corresponds to the $^5D_4 \rightarrow {}^7F_5$ transition, and the peaks at $\lambda = 586$ and 623 nm correspond to the $^5D_4 \rightarrow {}^7F_4$ and $^5D_4 \rightarrow {}^7F_3$ transitions, respectively. The effective lifetime of 3.8 ms is from the $^5D_4$ level (inset in Figure 2b) with an estimated quantum yield of 76% based on the radiative lifetime of 4.9 ms.[7g]

Figure 3 shows the TEM image of silica-coated LaF_3:Nd nanoparticles after being heated at 800°C for 12 h. The

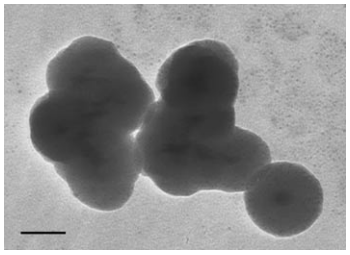

Figure 3. TEM image of silica-coated LaF_3:Nd nanoparticles, before surface modification, after being heated at 800°C. Scale bar = 20 nm.

beads have an average, slightly contracted shell thickness of ≈ 15 nm (± 5 nm) with no observable effects of particle fusing. Figure 4a shows the emission spectrum of the silica-coated LaF_3:Nd nanoparticles, in which the emission peaks at $\lambda = 870$, 1070 and 1330 nm are from $^4F_{3/2}$ transitions to $^4I_{13/2}$, $^4I_{11/2}$ and $^4I_{9/2}$, respectively, with an effective luminescent lifetime of 0.170 ms (inset in Figure 4a), suggesting a quantum yield of several tens of percent. Due to the ability of lanthanide ions to be excited indirectly through the sensitised emission of another lanthanide ion, Figure 4b shows the emission spectrum of silica-coated LaF_3:Yb,Er nanoparticles through sensitised emission from the Yb^{3+} to the Er^{3+} ions, by direct excitation of the Yb^{3+} ions at $\lambda = 940$ nm. The importance of this spectrum demonstrates that though Er^{3+} has no absorption lines at this wavelength, this process results in the simultaneous, very weak emission of Yb^{3+} at $\lambda =$ 980 nm (attributed to the $^2F_{5/2} \rightarrow {}^2F_{7/2}$ transition) and the sensitised emission of the Er^{3+} ions at $\lambda = 1540$ nm ($^4I_{13/2} \rightarrow {}^4I_{15/2}$ transition), with an effective lifetime of 1.8 ms for the $^4I_{13/2}$ level (inset in Figure 4b) suggesting a quantum yield of 10–20%.

The emission spectrum of the silica-coated LaF_3:Yb,Er nanoparticles heated at 800°C (Figure 5a) shows the upconversion emission of the Er^{3+} ions, with the peaks at $\lambda = 515$, 540 and 660 nm being assigned to the $^2H_{11/2} \rightarrow {}^4I_{15/2}$, $^4S_{3/2} \rightarrow {}^4I_{15/2}$ and $^4F_{9/2} \rightarrow {}^4I_{15/2}$ transitions, respectively. Furthermore, Figure 5b demonstrates the upconversion-emission spectrum of heated silica-coated LaF_3:Yb,Tm nanoparticles, in which the emission band around $\lambda = 800$ nm is a result of the $^3H_4 \rightarrow {}^3H_6$ transition of Tm^{3+} ions. Moreover, a weak Tm^{3+} emission band at $\lambda = 475$ nm was observed and assigned to the $^1G_4 \rightarrow {}^3H_6$ transition (inset in Figure 5b), and is also a result of the upconversion process. Preliminary results into the mechanism of the upconversion process suggest that it is oc-

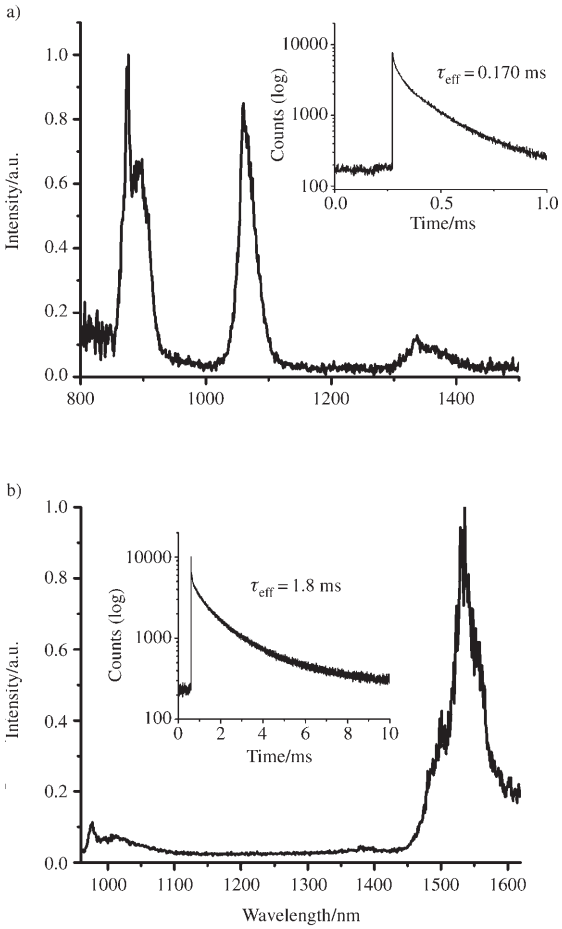

Figure 4. a) Emission spectra of silica-coated LaF_3:Nd nanoparticles after being heated at 800°C ($\lambda_{ex} = 514$ nm). Inset: decay curve for silica-coated LaF_3:Nd nanoparticles, before surface modification, after being heated at 800°C ($\lambda_{ex} = 514$ nm, $\lambda_{em} = 1070$ nm). b) Emission spectra of silica-coated LaF_3:Yb,Er nanoparticles after being heated at 800°C ($\lambda_{ex} = 980$ nm). Inset: decay curve for silica-coated LaF_3:Yb,Er nanoparticles, before surface modification, after being heated at 800°C ($\lambda_{ex} = 940$ nm, $\lambda_{em} =$ 1540 nm).

curring through energy transfer (ET) rather than an excited-state absorption (ESA) or photoavalanche (PA) process.[18b] Shown in Figure 6 are the schematic diagrams of the energy levels and possible energy-transfer processes of the silica-coated LaF_3:Yb,Er and LaF_3:Yb,Tm nanoparticles. The emissions of Er^{3+} at $\lambda = 510$, 540 and 660 nm are due to two-photon processes. The emission of Tm^{3+} at $\lambda = 795$ nm is a two-photon process and that at $\lambda = 475$ nm is a three-photon process.

To test the ability of the core–shell silica nanoparticles to be bound to a biochemical system, surface modification of the silica shell with biotin was used as a model for nanoparticle binding with FITC–avidin, and the extent of binding was monitored by the FITC emission intensity. Due to the biologically inert nature of silica, the shell had to be modified first in a two-step process in order to impart biotin activity (see Scheme 1).

The emission spectrum of the bioconjugation of silica-coated LaF_3:Tb nanoparticles to FITC–avidin, which is

 © 2006 Wiley-VCH Verlag GmbH & Co. KGaA, Weinheim

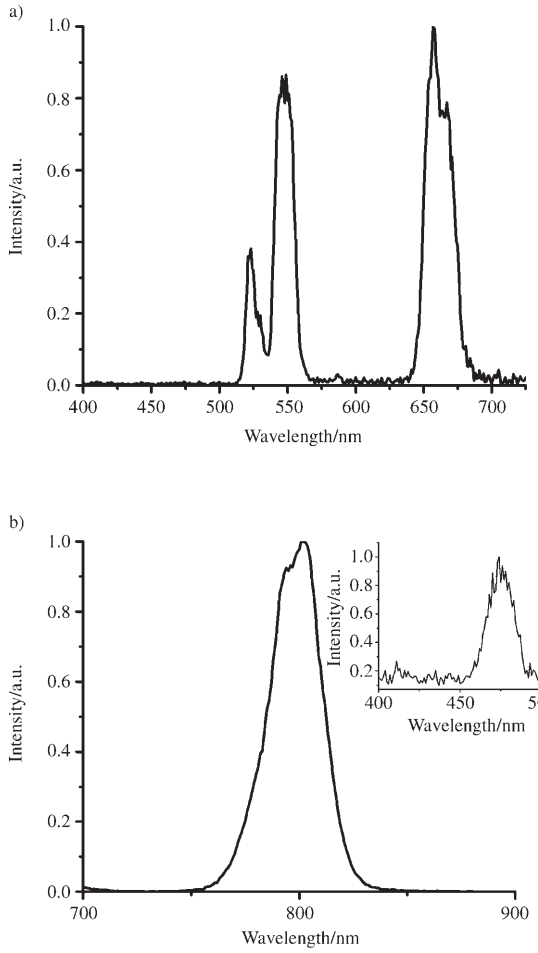

Figure 5. a) Upconversion-emission spectra of silica-coated LaF_3:Yb,Er nanoparticles after being heated at 800 °C ($\lambda_{ex}=980$ nm). b) Upconversion-emission spectra of silica-coated LaF_3:Yb,Tm nanoparticles after being heated at 800 °C ($\lambda_{ex}=980$ nm). Inset: upconversion-emission spectra of silica-coated LaF_3:Yb,Tm nanoparticles, before surface modification, after being heated at 800 °C ($\lambda_{ex}=980$ nm).

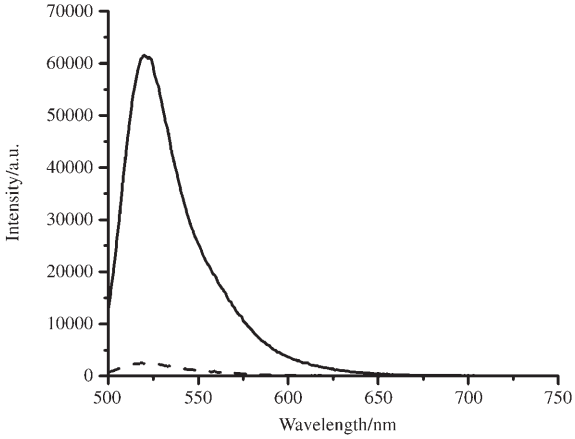

Figure 7. Emission spectra of silica-coated LaF_3:Tb nanoparticles after bioconjugation with FITC–avidin beads: ——=specific binding; – – –= nonspecific binding. ($\lambda_{ex}=485$ nm; excitation source: Xe lamp.)

shown with the spectrum for non-biotinylated particles as control particles, is shown in Figure 7. The emission spectrum shows an approximate 25-fold increase in FITC signal relative to the control particles, clearly proving that specific binding of avidin to the silica particles has been achieved, and that the signal from the control particles is likely a result of some physical adsorption of avidin onto the particles in a negligible amount. This is a conservative estimate because control tests with APTES-modified beads showed that the nonspecific binding is about twofold less than that with the unmodified beads. This result is, however, superior to the monolayer-stabilised Ln^{3+}-doped LaF_3 nanoparticles previously reported by us.[10] Our previous work has shown that coating the surface of LaF_3:Ln^{3+} nanoparticles with poly(ethylene glycol)-based ligands minimised the effects of nonspecific binding, and we expect the same result with our current silica particles.[10] The effect of nanoparticle aggregation after bioconjugation has not yet been studied on our silica-coated nanoparticles. No terbium emission was observed because of the low absorption coefficient of Tb^{3+} ions relative to FITC and the low excitation power of the 450 W Xe lamp. Figure 8 shows the Tb^{3+} emission spectrum of the particles excited with high excitation power, in which the sharp $\lambda=544$ nm peak of Tb^{3+} is visible on top of the FITC signal, with an effective luminescent lifetime of 3.2 ms (inset in Figure 8), which is in agreement with that of the unmodified and APTMS-modified particles. The same binding experiments were carried out on silica-coated LaF_3:Nd nanoparticles resulting in a similar increase in FITC emission relative to the control particles (Figure 9). Figure 10 shows the emission spectrum of the silica-coated

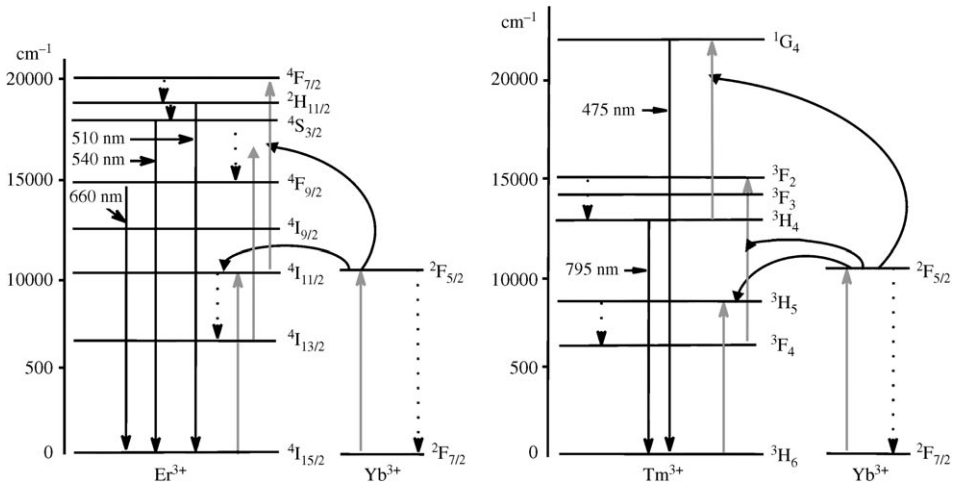

Figure 6. Energy levels of Er^{3+}, Tm^{3+} and Yb^{3+} ions as well as the upconversion mechanisms based on ref. [9].

 © 2006 Wiley-VCH Verlag GmbH & Co. KGaA, Weinheim

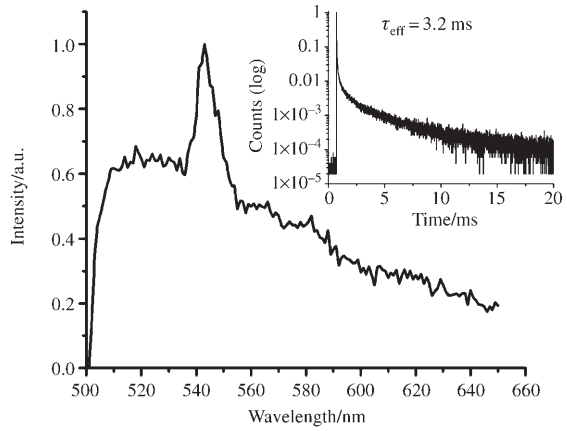

Figure 8. Emission spectra of FITC–avidin-bound silica-coated LaF_3:Tb nanoparticles in 10 mM phosphate-buffered saline solution (λ_{ex} = 485 nm; excitation source: OPO). Inset: decay curve of Tb^{3+} (λ_{ex} = 485 nm, λ_{em} = 542 nm). The effective lifetime was calculated by neglecting the initial part of the decay curve (0–0.8 ms), which is from FITC.

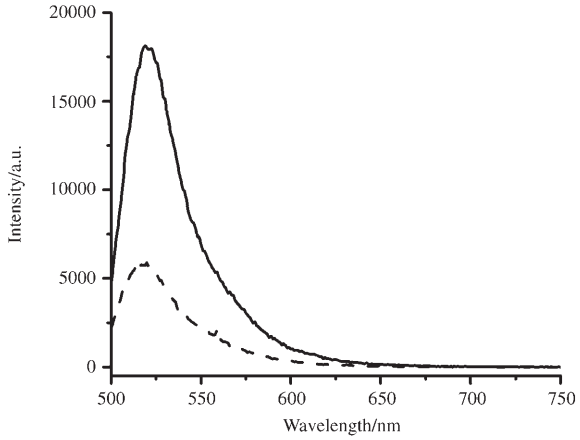

Figure 9. Emission spectra of silica-coated LaF_3:Nd nanoparticles after bioconjugation with FITC–avidin beads in 10 mM phosphate-buffered saline solution: ——= specific binding; – – – = nonspecific binding. (λ_{ex} = 485 nm; excitation source: Xe lamp.)

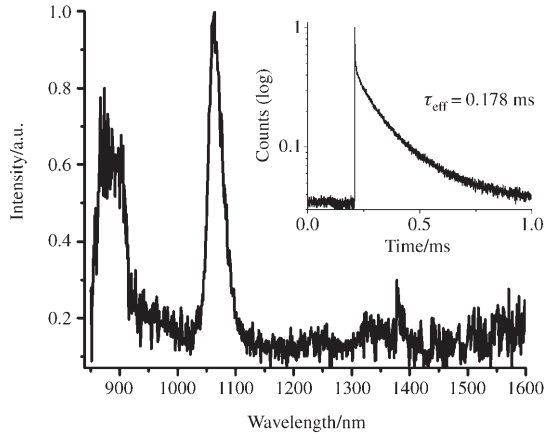

Figure 10. The emission spectra of FITC–avidin-bound silica-coated LaF_3:Nd nanoparticles in 10 mM phosphate-buffered saline solution (λ_{ex} = 514 nm; excitation source: OPO). Inset: decay curve of Nd^{3+} (λ_{ex} = 514 nm, λ_{em} = 1070 nm).

LaF_3:Nd nanoparticles, showing the characteristic peaks at λ = 870, 1064 and 1330 nm, with an effective luminescent lifetime of 0.178 ms (inset in Figure 10), which is in agreement with that of the unmodified particles. The formation of the silica coating over the LaF_3:Nd and LaF_3:Yb,Er nanoparticles improved the NIR luminescence significantly compared with our previously reported citrate and 2-aminoethylphosphate-stabilised LaF_3:Nd nanoparticles, by minimising the solvent quenching effect.[10]

Conclusion

In conclusion, a general and facile method for the production of silica-coated LaF_3:Ln^{3+} nanoparticles with a uniform size distribution and their bioconjugation to FITC–avidin have been successfully demonstrated. A wide range of emission lines (λ = 450–1650 nm) by up- and downconversion processes have been achieved by doping with different lanthanide ions. In particular, the excitation with λ = 980 nm light on codoped silica-coated LaF_3:Yb,Tm nanoparticles resulted in an emission at λ = 800 nm by upconversion processes, which has potential for biological applications. The surface modification of silica-coated nanoparticles with APTMS, followed by biotin for biotin–avidin binding, resulted in a 25-fold increase in the FITC signal relative to non-biotin-functionalised silica-coated nanoparticles.

Experimental Section

Chemicals of the highest purity were obtained from Aldrich and used without further purification. The FITC–avidin was obtained from Invitrogen and used as received. All water used was distilled. All nanoparticles were made with LaF_3 and were doped with the respective atom percentage relative to the total Ln^{3+} amount.

Synthesis of nanoparticles: We have used our earlier reported procedure to prepare the citrate-stabilised LaF_3:Ln^{3+} nanoparticles.[18]

Synthesis of silica-coated LaF_3:Ln^{3+} nanoparticles: Citrate-stabilised LaF_3:Ln^{3+} nanoparticles (50 mg) dissolved in distilled water (1.44 mL) were added to an ethanol (20 mL) and 30 % NH_4OH (0.4 mL) mixture. Tetraethyl orthosilicate (TEOS, 1.2 mL) was then added to the above mixture. The mixture was stirred for 60 min. The white silica beads were centrifuged, and washed with ethanol several times. The silica beads were then dried under vacuum. The silica-coated LaF_3:Nd, LaF_3:Yb,Er and LaF_3:Yb,Tm nanoparticles were heated at 800 °C for 12 h in air.

Surface modification of the silica-coated LaF_3:Ln^{3+} nanoparticles with APTMS: Silica-coated LaF_3:Ln^{3+} nanoparticles (10 mg) were suspended in ethanol (10 mL), followed by the addition of APTMS (0.5 mL, 2 mmol) and stirred for 24 h at room temperature. The particles were isolated and purified by means of centrifugation, washed three times with ethanol and dried under reduced pressure.

Biotinylation of silica-coated LaF_3:Ln^{3+} nanoparticles: APTMS-modified silica-coated LaF_3:Ln^{3+} nanoparticles (10 mg) were suspended in DMSO (2 mL), followed by the addition of (+)-biotin–*N*-hydroxysuccinimide ester (10 mg, 0.03 mmol) and stirred for 1.5 h at room temperature. The particles were isolated and washed by centrifugation, washed once with water and three times with ethanol and dried under reduced pressure.

Biotin–FITC–avidin binding: Amine-modified silica-coated LaF_3:Ln^{3+} nanoparticles (10 mg) were suspended in 10 mM phosphate-buffered saline (10 mL, pH 7.4), followed by the addition of FITC–avidin (0.4 mL)

 © 2006 Wiley-VCH Verlag GmbH & Co. KGaA, Weinheim

(final avidin concentration of 0.1 mg mL^{-1}) and stirred for 2.5 h at room temperature. The particles were isolated and purified by centrifugation, washed five times with 10 mM phosphate-buffered saline solution and re-suspended in 10 mM phosphate-buffered saline solution (10 mL).

Characterization of silica-coated LaF_3:Ln^{3+} nanoparticles

Luminescence studies: Downconversion fluorescence analyses were carried out by using an Edinburgh Instruments FLS 920 fluorescence system, which was equipped with a CW 450 W xenon arc lamp, the light of which was passed through a M300 single-grating monochromator, and a 10 Hz Q-Switched Quantel Brilliant 355 II laser system, pumped by a Nd:YAG laser, attached to an optical parametric oscillator (OPO) with an optical range of $\lambda = 410$–2200 nm. The excitation source used for up-conversion was a Coherent two-pin 980 nm CW semiconductor diode laser with maximum power, P_{max}, of 800 mW at 1000 mA. A 100 μm core fibre was coupled (pigtailed) to the diode laser. A red-sensitive Peltier-cooled Hamamatsu R955 photomultiplier tube (PMT), with a photon-counting interface, was used for analyses between $\lambda = 200$ and 850 nm, and an N_2-cooled (−80 °C) Hamamatsu R5509 PMT was used for analyses between $\lambda = 800$ and 1700 nm. All emission analyses in the visible region were measured with a 1 nm resolution. All emission analyses in the near-infrared region were measured with a 10 nm resolution. All spectra were corrected for detector sensitivity. Lifetime analyses for all nanoparticles were carried out by exciting the solution with a 10 Hz Q-Switched Quantel Brilliant 355 II laser system, pumped by an Nd:YAG laser, with an optical range from $\lambda = 410$ to 2200 nm, and the emission was collected by using the respective detector mentioned above. Decay curves were measured with a 0.01 ms lamp trigger delay for the R955 PMT. Effective lifetimes were calculated by using Origin 7 software. The effective lifetimes were calculated by using Origin 7 software based on Equation (1):[20]

$$\tau_{\text{eff}} = \frac{\int_0^\infty tI(t)\mathrm{d}t}{\int_0^\infty I(t)\mathrm{d}t} \quad (1)$$

All luminescence studies were carried out with samples as dry powders for unmodified, heated (800 °C) silica-coated LaF_3:Nd, LaF_3:Er, LaF_3:Yb,Er and LaF_3:Yb,Tm nanoparticles. The other samples were analysed as buffer solutions.

Transmission electron microscopy (TEM): TEM analyses of the silica-coated LaF_3:Ln^{3+} nanoparticles were carried out by using a Hitachi H-7000 microscope, operated at 100 kV. Around 1–2 mg of sample was dispersed in 5 mL of ethanol and a drop of this mixture was evaporated on a carbon-coated 300 mesh copper grid. Around 45 images were recorded from different regions of the same sample and an average particle size was obtained based on a minimum of 100 particles.

Acknowledgements

The National Research and Engineering Council (NSERC) of Canada, the Canada Foundation for Innovation (CFI) and the British Columbia Knowledge Development Fund (BCKDF) of Canada are gratefully acknowledged for financial support.

[1] a) M. J. Bruchez, M. Moronne, P. Gin, S. Weiss, A. P. Alivisatos, *Science* **1998**, *281*, 2013–2016; b) W. C. W. Chan, S. Nie, *Science* **1998**, *281*, 2016–2018.

[2] a) K. L. Holmes, L. M. Lantz, *Methods Cell Biol.* **2001**, *63*, 185–204; b) P. R. Banks, D. M. Paquette, *Bioconjugate Chem.* **1995**, *6*, 447–458.

[3] a) J. R. Taylor, M. M. Fang, S. Nie, *Anal. Chem.* **2000**, *72*, 1979–1986; b) R. C. Bailey, J. M. Nam, C. A. Mirkin, J. T. Hupp, *J. Am. Chem. Soc.* **2003**, *125*, 13541–13547; c) E. R. Goldman, E. D. Balighian, H. Mattoussi, M. K. Kuno, J. M. Mauro, P. T. Tran, G. P. Anderson, *J. Am. Chem. Soc.* **2002**, *124*, 6378–6382; d) J. K. Jaiswal, H. Mattoussi, J. M. Mauro, S. M. Simon, *Nat. Biotechnol.* **2003**, *21*, 47–51; e) S. J. Rosenthal, I. Tomlinson, E. M. Adkins, S. Schroeter, S. Adams, L. Swafford, J. McBride, Y. Wang, L. J. DeFelice, R. D. Blakely, *J. Am. Chem. Soc.* **2002**, *124*, 4586–4594.

[4] a) W. J. Parak, D. Gerion, T. Pellegrino, D. Znachet, C. Micheel, S. C. Williams, R. Boudreau, M. A. LeGros, C. A. Larabell, A. P. Alivisatos, *Nanotechnology* **2003**, *14*, 15–27; b) J.-M. Nam, S. I. Stoeva, C. A. Mirkin, *J. Am. Chem. Soc.* **2004**, *126*, 5932–5933; c) Y. Kobayashia, H. Katakamia, E. Minea, D. Nagaoa, M. Konnoa, L. M. Liz-Marzán, *J. Colloid Interface Sci.* **2005**, *283*, 392–396.

[5] F. Wang, W. B. Tan, Y. Zhang, X. Fan, M. Wang, *Nanotechnology* **2006**, *17*, R1–R13.

[6] a) C. L. Nehl, N. K. Grady, G. P. Goodrich, F. Tam, N. J. Halas, J. H. Hafner, *Nano Lett.* **2004**, *4*, 2355–2359; b) C. Loo, A. Lowers, N. Halas, J. West, R. Drezek, *Nano Lett.* **2005**, *5*, 709–711.

[7] a) J. W. Stouwdam, F. C. J. M. van Veggel, *Nano Lett.* **2002**, *2*, 733–737; b) J. W. Stouwdam, F. C. J. M. van Veggel, *Langmuir* **2004**, *20*, 11763–11771; c) V. Sudarsan, F. C. J. M. van Veggel, R. A. Herring, M. Raudsepp, *J. Mater. Chem.* **2005**, *15*, 1332–1342; d) F. Vetrone, J. C. Boyer, J. A. Capobianco, A. Speghini, A. M. Bettinelli, *J. Phys. Chem. B* **2003**, *107*, 1107–1112; e) A. Patra, C. S. Friend, R. Kapoor, P. N. Prasad, *Appl. Phys. Lett.* **2003**, *83*, 284–286; f) S. Heer, K. Kompe, H.-U. Gudel, M. Haase, *Adv. Mater.* **2004**, *16*, 2102–2105; g) M. H. V. Werts, R. T. F. Jukes, J. W. Verhoeven, *Phys. Chem. Chem. Phys.* **2002**, *4*, 1542–1548; h) K. Binnemans, R. Van Deun, C. Gorller-Walrand, J. L. Adam, *J. Non-Cryst. Solids* **1998**, *238*, 11–29.

[8] C. Feldmann, T. Justel, C. R. Ronda, P. J. Schmidt, *Adv. Funct. Mater.* **2003**, *13*, 511–516.

[9] J. C. Wright, *Top. Appl. Phys.* **1976**, *15*, 239–295.

[10] a) P. R. Diamente, F. C. J. M. van Veggel, *J. Fluoresc.* **2005**, *15*, 543–551; b) P. R. Diamente, R. D. Burke, F. C. J. M. van Veggel, *Langmuir* **2006**, *22*, 1782–1788.

[11] F. Meiser, C. Cortez, F. Caruso, *Angew. Chem.* **2004**, *116*, 6080–6083; *Angew. Chem. Int. Ed.* **2004**, *43*, 5954–5957.

[12] L. Wang, R. Yan, Z. Huo, L. Wang, J. Zeng, J. Bao, X. Wang, Q. Peng, Y. Li, *Angew. Chem.* **2005**, *117*, 6208–6211; *Angew. Chem. Int. Ed.* **2005**, *44*, 6054–6057.

[13] E. Beaurepaire, V. Buisette, M.-P. Sauviat, D. Giaume, K. Lahill, A. Mercuri, D. Casanova, A. Huignard, J.-L. Martin, T. Gacoin, J.-P. Boilot, A. Alexandrou, *Nano Lett.* **2004**, *4*, 2079–2083.

[14] C. Louis, R. Bazzi, C. A. Marquette, J.-L. Bridot, S. Roux, G. Ledoux, B. Mercier, L. Blum, P. Perriat, O. Tillement, *Chem. Mater.* **2005**, *17*, 1673–1682.

[15] P. Corstjens, M. Zuiderwijk, A. Brink, S. Li, H. Feindt, R. S. Neidbala, H. Tanke, *Clin. Chem.* **2001**, *47*, 1885–1893.

[16] a) H. Ow, D. R. Larson, M. Srivastava B. A. Baird, W. W. Webb, U. Wiesner, *Nano Lett.* **2005**, *5*, 113–117; b) L. M. Rossi, L. Shi, F. H. Quina, Z. Rosenzweig, *Langmuir* **2005**, *21*, 4277–4280.

[17] D. Gerion, W. J. Parak, S. C. Williams, D. Zanchet, C. M. Micheel, A. P. Alivisatos, *J. Am. Chem. Soc.* **2002**, *124*, 7070–7074.

[18] a) V. Sudarsan, S. Sivakumar, F. C. J. M. van Veggel, M. Raudsepp, *Chem. Mater.* **2005**, *17*, 4736–4742; b) S. Sivakumar, F. C. J. M. van Veggel, M. Raudsepp, *J. Am. Chem. Soc.* **2005**, *127*, 12464–12465.

[19] W. Stöber, A. Fink, E. J. Bohn, *J. Colloid Interface Sci.* **1968**, *26*, 62–69.

[20] C. Cannas, M. Casu, M. Mainas, A. Musinu, G. Piccaluga, S. Polizzi, A. Speghini, M. Bettinelli, *J. Mater. Chem.* **2003**, *13*, 3079–3084.

Received: February 17, 2006
Published online: June 1, 2006

 © 2006 Wiley-VCH Verlag GmbH & Co. KGaA, Weinheim